

# COSMIC RAYS

**To investigate the relative intensity of cosmic radiation as a function of zenith angle, and to check any E - W asymmetry.**

## **NOTE**

This experiment is usually "paired" with Rutherford Scattering as it can be performed whilst scattering counts for the latter experiment are accumulated.

## **INTRODUCTION**

Read Papers 1, 2 on the origin and properties of Cosmic Rays and the detector originally used in these experiments.

## **APPARATUS**

The detector used here differs from the one shown in Fig 4.6 in that a Perspex rod rather than water is used in the Cerenkov detector. In this detector, a flash of light is produced in the Perspex by Cerenkov radiation which occurs when the incoming particle exceeds the speed of light in the medium ( $\sim 2 \times 10^8 \text{ ms}^{-1}$  in Perspex). This "scintillation" is detected by a photomultiplier, the output of which goes to the amplifier/analyser. The analyser also contains a discriminator circuit (labelled E) which sets a minimum pulse height below which there is no output trigger pulse to the counter.

The E.H.T. to the photomultiplier is controlled by a separate power supply which is normally set at around 1.75 kV.

The zenith angle is adjusted by the control handle; a complete turn of the latter moves the zenith angle by  $6^\circ$ .

The apparatus should preferably be allowed 24 hours to warm up and "settle down".

## **MEASUREMENTS**

As with many nuclear physics experiments adjustments which eliminate noise pulses whilst retaining true events, is the initial aim. This is achieved by choice of discriminator setting.

## **DISCRIMINATOR ADJUSTMENT**

Obtain total counts over 100 seconds for values of discriminator (E) ranging from  $0.5 \rightarrow 5.0$  approx., with gain set at 300 and the fine control fully clockwise (set  $\Delta E$  at 9.5v). Do this both for zenith angle = 0 (vertically UP) and zenith angle =  $180^\circ$  (vertically DOWN). Plot bias curves (i.e. counts vs. discriminator) for each position on the same graph. This should yield curves similar to Fig. 4.7.

On the same graph plot also  $N = N_{\text{UP}} - N_{\text{DOWN}}$  which (assuming all the down counts,  $N_{\text{DOWN}}$  are noise) should give the true cosmic ray count.

Choose a discriminator value for which the noise is low, but for which not too many true counts N are lost.

**When resetting the timer unit, ensure that the Ratemeter display returns to ZERO!**

## **INTENSITY AS A FUNCTION OF ZENITH ANGLE. $\theta$**

Obtain counts for 200 seconds for  $\theta = -90^\circ$  (W) to  $+90^\circ$  (E) at  $6^\circ$  intervals. Obtain also the background count  $N_{\text{DOWN}}$  for 200 seconds, and subtract from all your readings to give a corrected count, N. Plot N vs.  $\theta$ . Compare with a  $\cos^2 \theta$  variation on the same graph (see Fig. 4.8). The variation cannot be truly  $\cos^2 \theta$  because there is an E - W asymmetry,  $\epsilon$ :

$$\epsilon = (N_W - N_E) / \frac{1}{2}(N_W + N_E)$$

Although  $\epsilon$  is a function of  $\theta$ , you will not have enough counts to determine its variation, so obtain an average value of  $\epsilon$  by taking  $N_E$  = all the readings to the east and  $N_W$  = all the readings to the west in the above formula. Calculate the error in  $\epsilon$ .

## Chapter 25

# Cosmic Rays

### 25.1 Discovery

As long ago as 1900, C. T. R. Wilson and others found that the charge on an electroscope always 'leaked' away in time, and this could never be prevented, no matter how good the insulation. When the properties of radioactive radiations were better known Rutherford showed that the rate of leakage was considerably reduced by shielding the electroscope with thick slabs of lead, but there was always a residual leakage of charge which could not be eliminated. It was thought therefore that the initial conduction in the enclosed gas was probably due to ionizing radiations from radioactive minerals in the ground. When it was shown that over the sea where mineral radioactive effects are negligible the rate of leakage was still pronounced and was only partially diminished by shielding it was concluded that the ionizing radiations were descending as well as ascending. The famous experiment of Hess in 1912 in which he sent up an ionization chamber in a balloon and found that the intensity of ionization actually increased up to a height of 5000 metres and then decreased again, showed beyond doubt that these ionizing radiations travel down to earth through the air. A further observation showed that the intensities were the same for night or day indicating that the origin of these radiations was not solar. Hess suggested therefore that these rays were of cosmic origin, and they were finally called 'cosmic rays' by Millikan in 1925.

Millikan and others conducted some early researches on cosmic rays and found that there were two components, soft and hard, and that the hard, or very penetrating component, was not fully absorbed by many feet of lead or even at the bottom of lakes as deep as 500 m. This showed that the energy of cosmic rays was many times that of any other natural or artificial radiation known at that time.

In 1927 Clay found that the intensity of cosmic rays depended upon latitude, being a minimum at the equator and a maximum at the poles. This is a geomagnetic effect supporting the suggestion that cosmic rays are charged particles entering the Earth's magnetic field from a great distance. At this stage the really intensive study of the properties of cosmic rays and their uses in nuclear physics had really begun.

## 25.2 Nature of Cosmic Rays

Primary cosmic rays have their origin somewhere out in space. They travel with speeds almost as great as the speed of light and can be deflected by planetary or intergalactic magnetic fields. They are unique in that a single particle can have an energy as high as  $10^{19}$  eV but the collective energy is only about 10 microwatts per sq. metre for cosmic rays entering the atmosphere, which is roughly equal to the energy of starlight. In starlight the energy of a single photon is only a few electron volts compared with the average for cosmic rays, of 6 GeV per particle where  $1 \text{ GeV} = 10^9 \text{ eV}$ .

The composition of cosmic rays entering the earth's atmosphere, is fairly well known from balloon experiments and it is found that these primary cosmic rays consist mainly of fast protons. There are very few positrons, electrons or photons, and the 'particle' composition is mainly 92% protons, 7%  $\alpha$ -particles and 1% 'heavy' nuclei, carbon, nitrogen, oxygen, neon, magnesium, silicon, iron, cobalt and nickel stripped of their electrons. The average energy of the cosmic ray flux is 6 GeV, with a maximum of about  $10^{10}$  GeV (compare this with 300 GeV, the maximum energy of the artificially accelerated particles). The radiation reaching the earth is almost completely isotropic.

As soon as the primary rays enter the Earth's atmosphere multiple collisions readily take place with atmospheric atoms producing a large number of secondary particles in showers. Thus when a primary proton strikes an oxygen or nitrogen nucleus a nuclear cascade results. These secondary atmospheric radiations contain many new particles, neutral and ionized, as well as penetrating photons, but little if any of the primary radiation survives at sea-level. Secondary cosmic rays at sea-level consist of about 75% muons and about 25% electrons and positrons, although some alpha particles, gamma photons and neutrons may be present in negligible quantities. The muon will be described later.

The collision cross-sections for the primary component of cosmic rays are of the order of  $10^{-1}$  barns and the mean free path for a collision process at the top of the atmosphere may be as high as several kilometres. The new particles produced after primary collisions give in their turn more secondary radiations by further collisions until a cascade of particles has developed, increasing in intensity towards the Earth. This is shown diagrammatically in Fig. 25.1 and an actual photograph of a cascade shower deliberately produced in lead is shown in Fig. 25.2.

The energy spectrum of the primary cosmic rays ranges from  $10^9$  eV to about  $10^{19}$  eV and can be written  $\frac{dN}{dE} = K(E + m_0 c^2)^{-\gamma}$ , where  $N$  is the number of nuclei with a kinetic energy per nucleon  $> E$  (in GeV),  $m_0 c^2$

TABLE 25.1  
Composition of Primary Cosmic Rays Entering Earth's Atmosphere

Nucleus	% Composition	Energy range GeV/nucleon	Flux, i.e. no. of particles $m^{-2}s^{-1}$ per unit solid angle
H	92	2—20	$4000 E^{-8/7}$
He	7	1.5—8	$460 E^{-7/4}$
Li Be B	0.18	—	$12 E^{-7/4}$
C N O F	0.36	3—8	$24 E^{-7/4}$
Ne and beyond	0.15	3—8	$16 E^{-2}$

$E$  is the total energy per nucleon in GeV.

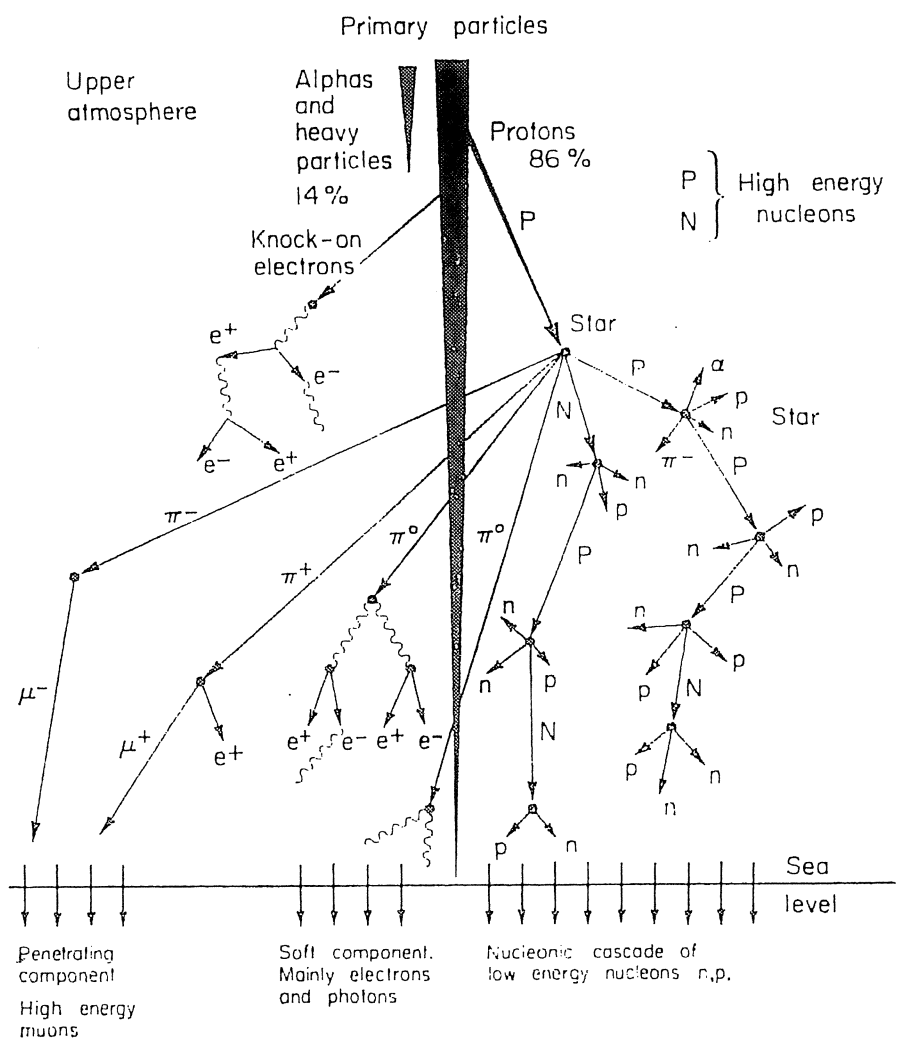


Fig. 25.1 Secondary products from a primary cosmic ray particle collision in the atmosphere.

is the nucleonic rest energy and  $K$  and  $\gamma$  are constants for a given cosmic ray component. This is represented in Table 25.1. Above 1.5 GeV per nucleon the cosmic ray intensity is fairly steady with time, with flux values in space of about

Protons	1500 nuclei/ $m^2 s$ unit solid angle
$\alpha$ -particles	90 nuclei/ $m^2 s$ unit solid angle
'Heavies'	10 nuclei/ $m^2 s$ unit solid angle

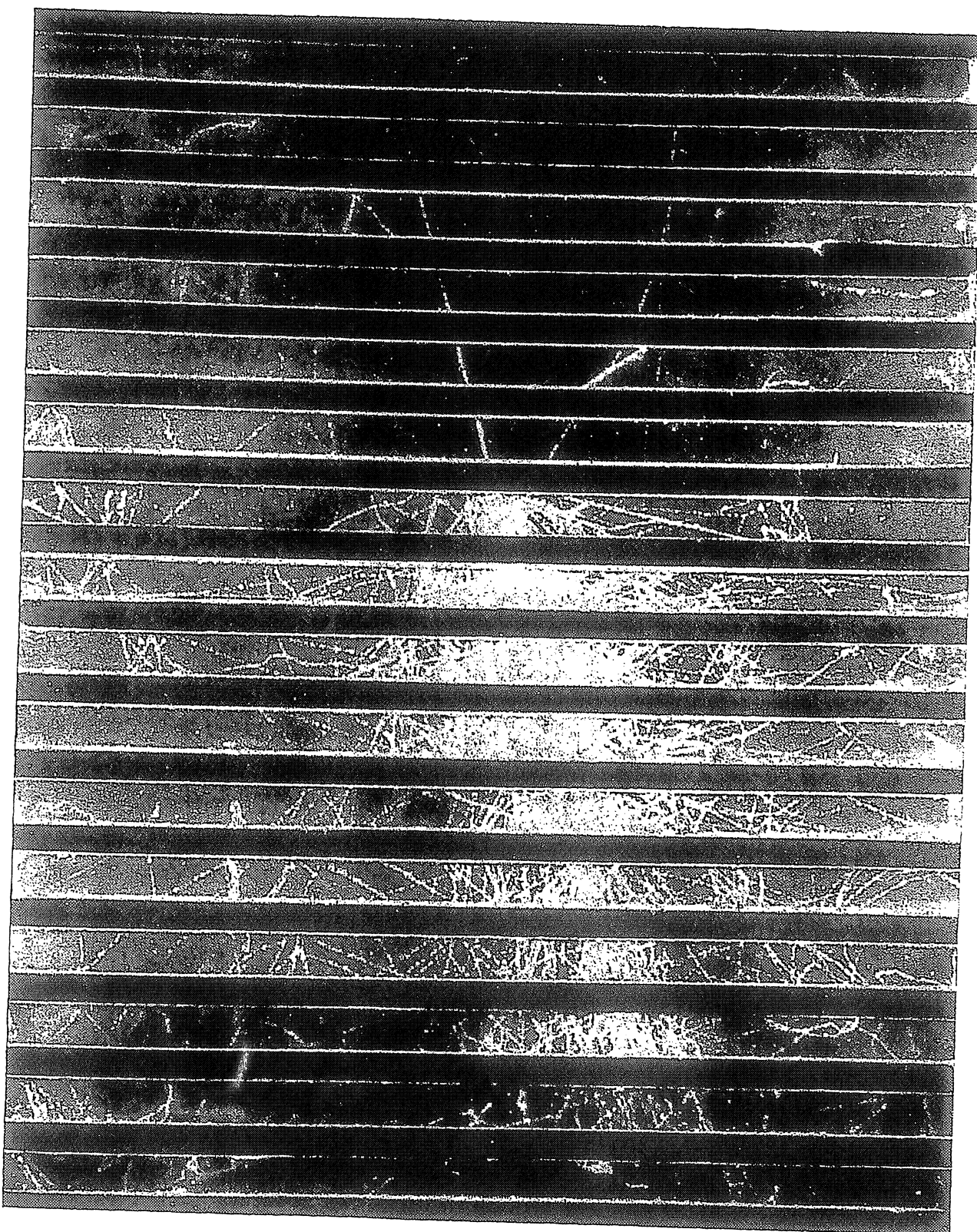


Fig. 25.2 Cascade shower produced in lead plates. Cloud chamber photograph. (From Rochester and Wilson, *Cloud Chamber Photographs of the Cosmic Radiation*. Pergamon, 1952.)

At lower energies the cosmic ray intensity is not constant with time but depends on the activity of the sun. It is found that during periods of high sunspot activity the cosmic ray intensity is low, presumably due to the trapping of the charged primaries high above the Earth by the increased magnetic field of the sun at these times. Corresponding to the 11-year cycle of maximum sunspot activity there is therefore a cycle of minimum cosmic ray intensity.

### 25.3 The Origin of Cosmic Rays

A recent observation on cosmic ray intensities showed that the sun itself must actually be the source of at least some of the low energy primaries, since at times of solar flares the cosmic ray intensity increased. However, this can only account for a small fraction of the total, and since cosmic rays are nearly isotropic around the earth their origin in such a 'point source' as the sun is precluded and we must look much further into the depths of space.

An interesting feature of the composition of the primary rays is the existence of heavy nuclides up to atomic masses of about 60, and the fact that the distribution of the elements in cosmic rays shows a similar trend to that in the sun, stars, nebulae and in the non-volatile parts of meteorites, although the primary cosmic radiations are significantly richer in heavy nuclei compared with the general matter of the universe. This seems to indicate a cosmic ray origin in which matter is present and where the conditions are of relatively low energy (compared with cosmic ray energies) possibly in supernovae explosions.

Fermi suggested that the cosmic rays have their origin in interstellar space and are accelerated to high energies, as they stream through the arms of a galaxy, by the associated galactic magnetic field which is about  $10^{-9}$  tesla or 1 nT. The cosmic ray particle is injected into the galactic magnetic field from the surface of a star with an appreciable initial energy and is caused to spiral in this field. It will eventually 'collide' with another region of high magnetic field which is approaching it with a high velocity. The cosmic ray particle is reflected or repelled with increased energy since the magnetic field is moving towards it. When a cosmic ray particle is trapped between two such fields it gains energy by multiple repulsions and the more energetic particles of the distribution finally escape into space with a high velocity of projection. This model is not unlike the 'mirror'-machine discussed in the previous chapter. The trapping and ejecting mechanism can be repeated until the particle reaches the solar system where it is observed.

It is concluded, therefore, that cosmic rays acquire their energies in the vicinity of magnetically active stars, especially supernovae. This is supported by the observations on radio stars which show intense radio noise

due to very fast electrons moving in magnetic fields suggesting that cosmic rays may also be associated with stellar events of great violence. Since the cosmic rays are pushed about in all directions by these great belts of stellar magnetic fields, in which they undergo multiple reflections and changes of direction, they surround the Earth isotropically so that the Earth can be regarded as a simple body in a whole sea of cosmic rays.

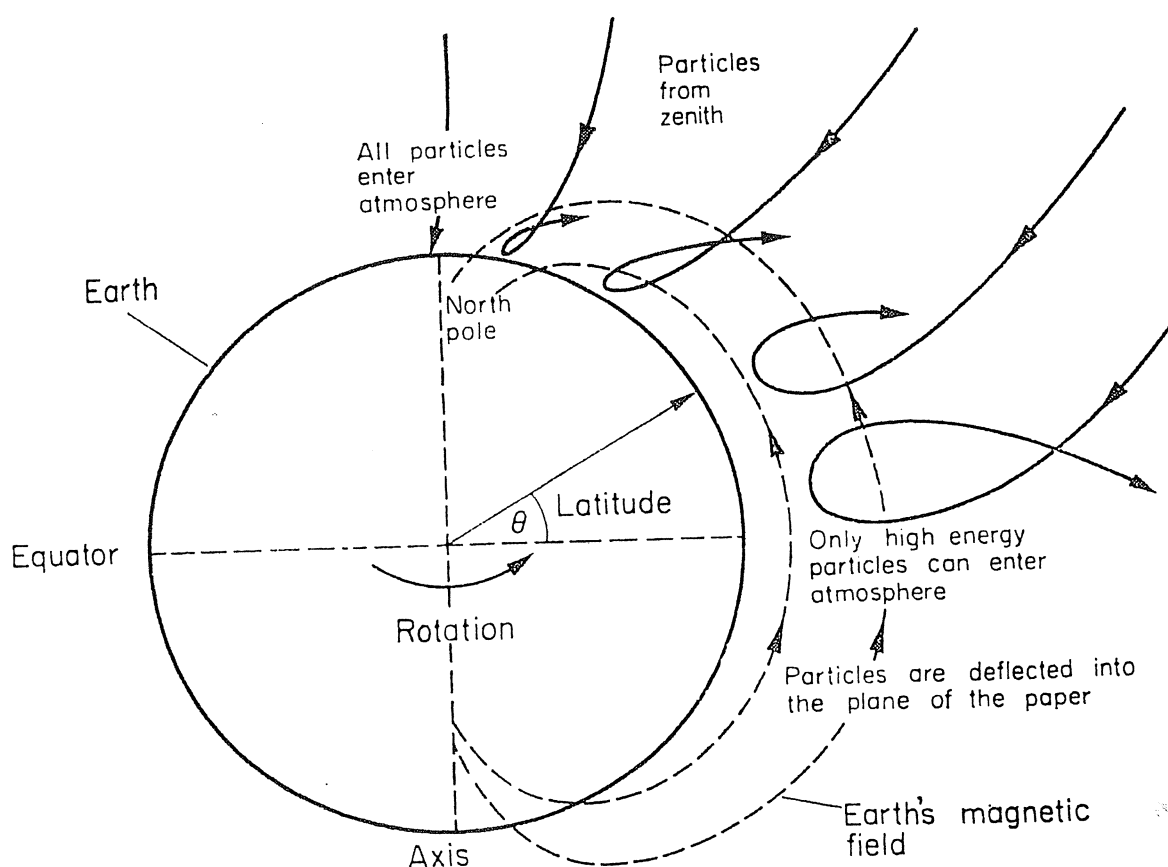


Fig. 25.3 Deflection of cosmic ray particles approaching from zenith showing action of Earth's magnetic field.

#### 25.4 Geomagnetic Effects

Compton and Millikan in 1935 carried out a world-wide survey of cosmic ray intensities and showed that the lines of equal cosmic ray intensity followed closely the Earth's geomagnetic latitude indicating that some, at least, of the primaries must be charged particles affected by the variations in the geomagnetic field.

The Earth has a magnetic moment of about  $10^{19}$  S.I. units with a magnetic field of flux density  $30 \mu\text{T}$  at the equator. As shown in Fig. 25.3 for the particles that enter the Earth's atmosphere 'vertically' and parallel to the geomagnetic lines of force at the poles, there is little interaction between the magnetic field and the charged particles near the poles. However, near the equator the magnetic field is perpendicular to the direction of the cosmic rays and the interaction is therefore much greater

so that the less energetic particles are deflected out of their original path. Only those exceeding a critical energy reach the Earth's surface. This critical energy is equivalent to a 'cut-off' in the energy spectrum, and depends on the latitude.

The minimum particle momentum, corresponding to the cut-off energy, is given by  $P_{\min} = 14.85 \cos^4 \lambda$  where  $\lambda$  is the magnetic latitude and the unit of momentum is  $\frac{\text{GeV}}{c}$

No particle below this limit can reach the Earth at a given latitude  $\lambda$  and the maximum value of  $P_{\min}$  is 14.85 at the equator and about 0.9 at  $\lambda = 60^\circ$ . It is probable that some of the low energy components in the primary radiations are trapped in the Earth's field at very high altitudes giving rise to the Van Allen radiation belts discovered in the American satellite experiments in 1958. These are toroidal-shaped regions containing circulating particles of low energy but high intensity. The axis of these belts coincides with the geomagnetic axis. See Fig. 25.4.

Since the main geomagnetic field is directed from south to north over the surface of the Earth, and assuming the primary particles are positively charged, the moving cosmic ray nuclei are deflected towards the east in accordance with the left hand motor rule. This gives an east-west effect in which the observed intensity of cosmic rays incident from the west is about 20% greater than that incident from the east. Thus slow cosmic ray particles come in more readily from the west than from the east. This asymmetry has been fully demonstrated experimentally, thus supporting the view that primary cosmic rays are positively charged and consist largely of protons.

### 25.5 Cosmic Rays at Sea-level

Secondary cosmic rays as measured at sea-level have a different distribution of particles from the primary rays. Very few primary ray protons reach sea-level where the penetrating or hard cosmic rays consist mainly of charged muons. We shall deal with the properties of these new sub-nuclear particles in the next chapter. It is sufficient to say here that upper atmospheric cosmic rays contain largely the so-called  $\pi$ -mesons or pions (mass  $273 m_e$ ) and  $\mu$ -mesons or muons (mass  $207 m_e$ ) of both signs. There are further secondaries, positrons, electrons and photons occurring in showers of innumerable particles. These make up the soft component, being absorbed by 100–200 mm of lead. At sea-level muons and electrons of both signs predominate.

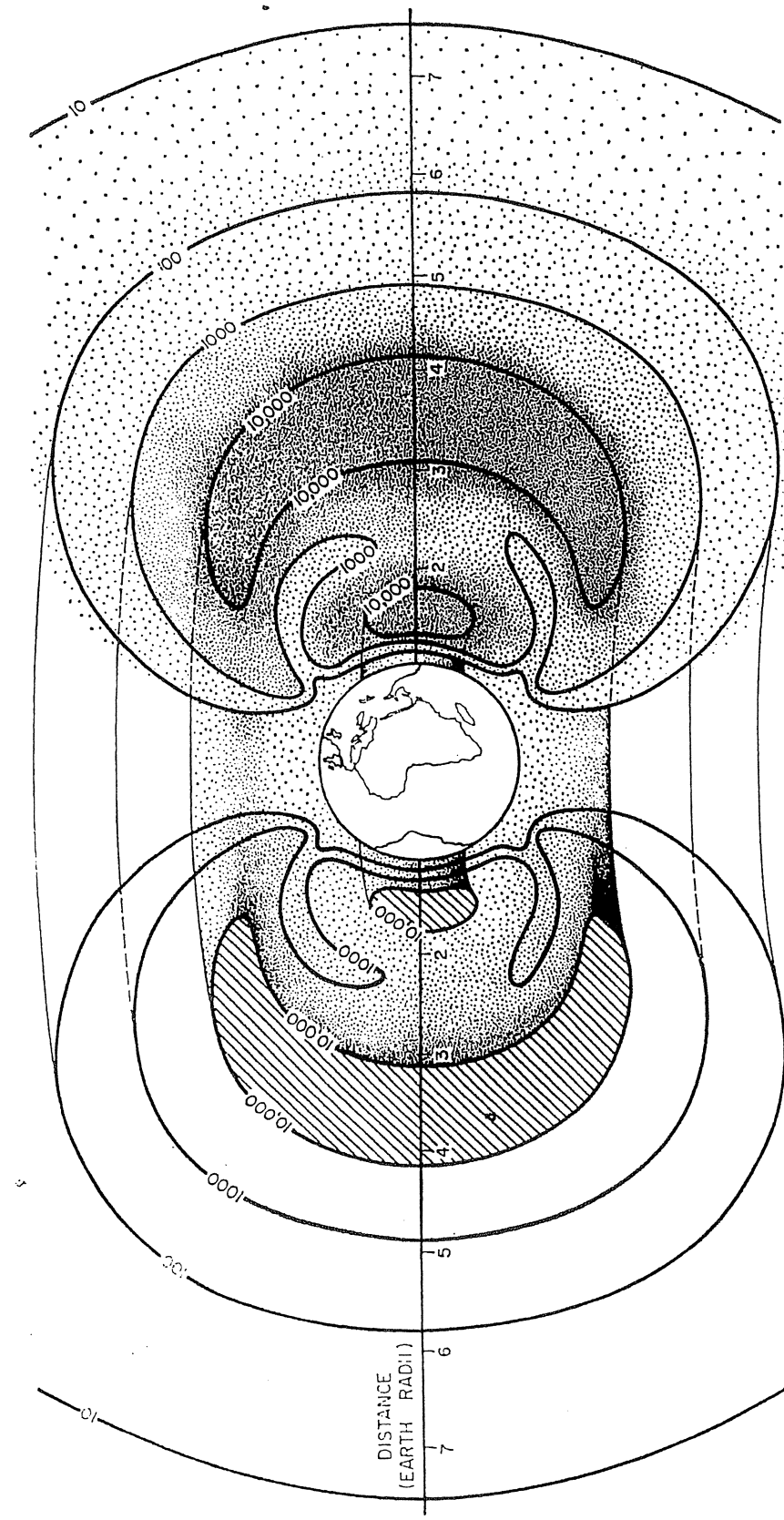


Fig. 25.4 Structure of radiation belts revealed by contours of radiation intensity (black lines) is shown schematically by shading (left); dots (right) suggest distribution of particles in the two belts. Contour numbers give counts per second; horizontal scale shows distance in Earth radii (about 4000 miles) from the centre of the Earth. Particles in the inner belt may originate with the radioactive decay of neutrons liberated in the upper atmosphere by cosmic rays: those in the outer belt probably originate in the sun. (From *Scientific American*, J. A. Van Allen, March, 1959, Vol. 200, No. 3, p. 39.)

## Geomagnetic Effects on the Sea Level Cosmic Rays

We have seen that only comparatively high energy primaries ( $\geq 10$  GeV) produce charged secondaries which are able to arrive at sea level before being absorbed. This means that the geomagnetic

effects will be much less at sea level than at high altitudes because it is the low energy primaries that are most affected by the earth's field.

The form of the variation of vertical intensity with latitude is very similar at all altitudes, with the intensity increasing with latitude in going from the equator to latitude  $60^\circ$  or so where the 'knee' occurs. At sea level the maximum variation in flux is only 14 per cent whereas at 4360 m the variation is 33 per cent and, as has been seen in Chapter 6 (Table 6), the variation near the top of the atmosphere amounts to a factor of 10. These variations are accounted for quite adequately by theory.

If a simple three-fold Geiger telescope is set up in the laboratory and measurements made on the variation of rate with angle to the vertical (zenith angle), it will be found that there is a difference between the rates when measured with eastward and westward inclinations. This phenomenon is called the east-west effect and has been known for many years. The variation is represented in Fig. 54. It is usual to define the east-west effect as

$$\epsilon = \frac{I_w(\theta) - I_e(\theta)}{\frac{1}{2}[I_w(\theta) + I_e(\theta)]}$$

where  $I_w(\theta)$  and  $I_e(\theta)$  are the intensities at zenith angle  $\theta$  towards the west and east, respectively. The main results that are found are that  $\epsilon$  increases with increasing altitude and decreasing latitude, and that it increases with zenith angle up to about  $60^\circ$ , above which it falls off. Typical values for the maximum values of  $\epsilon$  ( $\theta \sim 60^\circ$ ) at sea level are:  $\epsilon \sim 0.15$  at the geomagnetic equator,  $\sim 0.07$  at  $\lambda = 20^\circ$ ,  $\sim 0.05$  at  $\lambda = 30^\circ$ , and  $\epsilon \sim 0.02$  at  $\lambda = 50^\circ$ .

The explanation of the effect in physical terms is quite simple but the mathematical derivation is rather complicated. Briefly, since the primary radiation is entirely positively charged there is a higher cut-off rigidity towards the east than towards the west and both rigidities increase with decreasing latitude. As we have already seen (Fig. 30, page 73) the rigidities at the equator are 60 GV and 10 GV respectively for the special case of  $\theta = 90^\circ$ ; i.e. horizontal particles. At any given latitude the energy lost by the secondaries in getting through the atmosphere increases with increasing  $\theta$ , i.e. increasing path length in the atmosphere. This means that the energy of the primaries responsible for generating the particles arriving at sea level increases with increasing  $\theta$ . Now the difference in the rigidities between east and west increases with  $\theta$  so that there are two competing effects occurring, the increasing difference in

rigidities causing an increase in  $\epsilon$  and the increasing mean energy trying to produce a decrease in  $\epsilon$ . The result is that  $\epsilon$  goes through a maximum value in the region of  $\theta = 60^\circ$ .

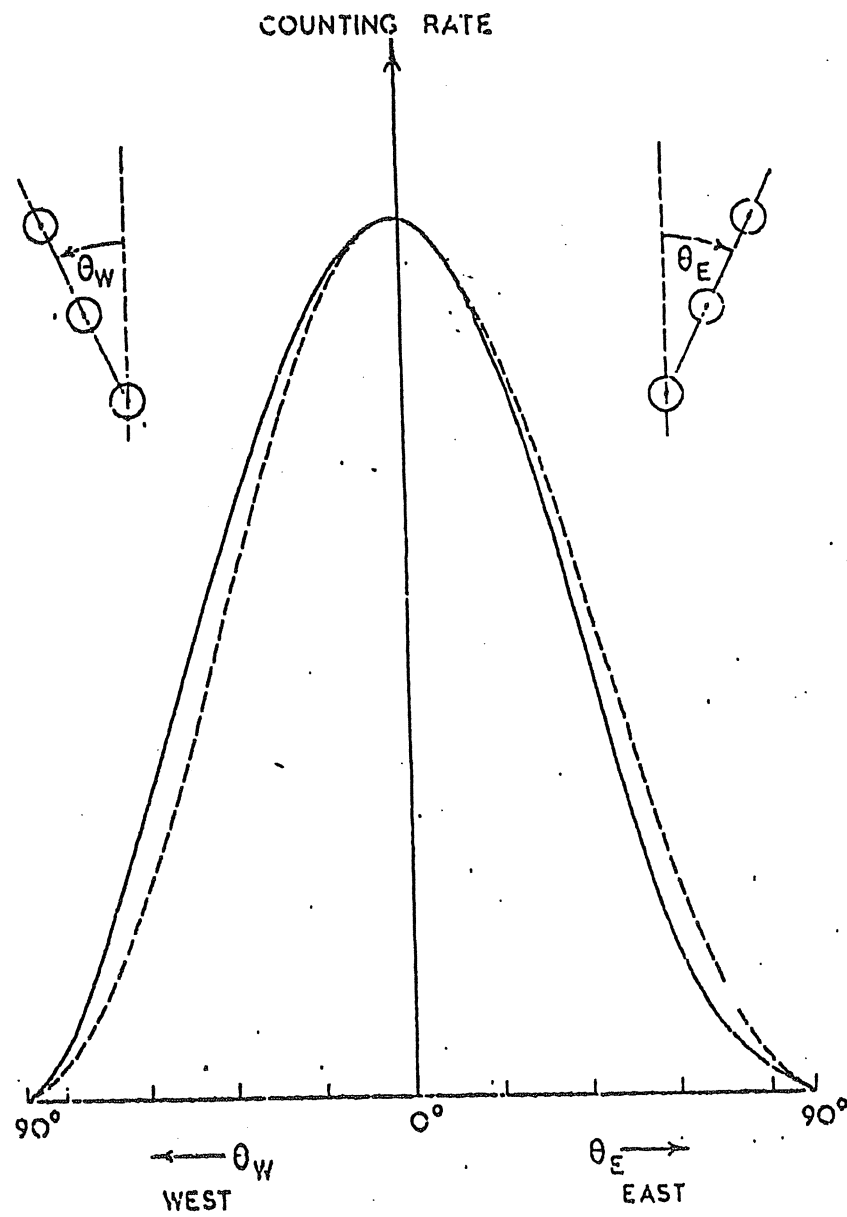


FIG. 54. EAST-WEST EFFECT. THE VARIATION OF COUNTING RATE OF A THREE-FOLD COUNTER TELESCOPE WITH ZENITH ANGLE.  
(The dotted curve is symmetrical with respect to  $\theta=0^\circ$ ).

The first clear evidence that single fast particles could be detected at high efficiency with a photomultiplier, was obtained by Jelley (1951) who used the simple water detector shown in Fig. 4.6. This experiment was also the first in which particles other than electrons were used to produce Čerenkov radiation.\* The detector was first operated in coincidence with a tray of Geiger counters to select cosmic-ray particles

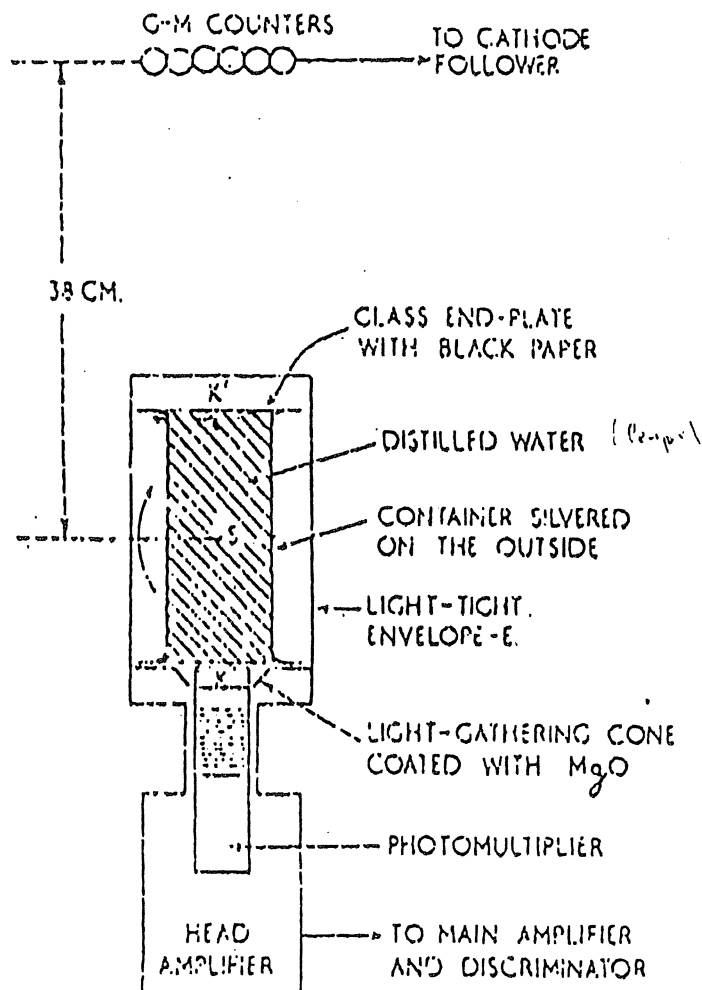


FIG. 4.6. The water detector used by Jelley (1951) to count single cosmic-ray  $\mu$ -mesons.

near the zenith. Since nearly all the particles are travelling in a downward sense through the apparatus, it follows that the Čerenkov radiation will also be directed downwards. The coincidence rate would thus be expected to be higher when the photomultiplier was in the position  $K$  below the container than when it was above, in position  $K'$ .

To investigate these coincidences, runs were done at different settings of the bias on a discriminator following the amplifier, with the phototube alternately in positions  $K$  and  $K'$ ; this was carried out by (ii)

rotating the whole detector about its mid-point  $S$ . Allowance was made for chance-rate and effects due to the particles traversing the photomultiplier; the latter were measured by repeating the runs with the container empty. Ratios of the counting rates (due to the water alone), for the phototube in position  $K$  and then in position  $K'$ , of  $3.25 \pm 0.32$ ,  $4.72 \pm 0.35$  and  $7.7 \pm 1.0$ , were obtained at bias levels of 2, 5 and 15 V respectively. With this arrangement the absolute efficiency of the detector was found to be  $\sim 50\%$  at a bias of 2 V. Confirmation that the observed directional feature of the light was genuine was obtained by replacing the water by a liquid scintillating medium which would give an isotropic light distribution. The corresponding ratio  $N(K)/N(K')$  at 2 V bias was then found to be  $1.26 \pm 0.06$ . That the effects were mostly due to  $\mu$ -mesons, the dominant component of cosmic-rays at sea-level, was shown by placing a 10 cm thick lead absorber above the apparatus, whereupon the rate dropped by  $\sim 20\%$ , which is approximately the electron contribution to the total cosmic-ray intensity at sea-level.

Jelley later found that at higher values of bias, at which the counting of dark-current pulses from the phototube was sufficiently reduced, the detector was sensitive to its orientation. It was then possible to detect particles with a good discrimination against background, without the necessity for the coincidence system, as revealed in the bias curves shown in Fig. 4.7. Curves (B) and (C) refer to the counting rates of the detector in the  $K$  and  $K'$  positions respectively, while curve (A) refers to the container empty. The ratio of the derived curves (D) and (E) for the water alone, shown inset, rises to an intensity ratio as high as 70/1 for the  $K$  and  $K'$  positions respectively. The directional characteristic of this simple cylindrical form of detector is shown in Fig. 4.8, where it is compared with the  $\cos^2\theta$  distribution, the accepted law of variation of  $\mu$ -meson intensity with zenith angle  $\theta$ .

Bassi (1951) attempted to determine the energy of cosmic-ray particles by measuring light intensity rather than emission angle, from the relation  $(dW'/dI) \propto (1 - 1/\beta^2 n^2)$ , equation (2.17). Using a detector similar to Jelley's, sandwiched between two Geiger counters, he obtained 100% efficiency for counting particles traversing the system. His efforts at measuring energies in this way were however defeated by statistical considerations. With a total flux of 3000 photons/particle (see equation 2.21) and a photocathode conversion efficiency of  $\sim 1$  electron/100 photons, the fluctuations on the 30 available electrons amount to

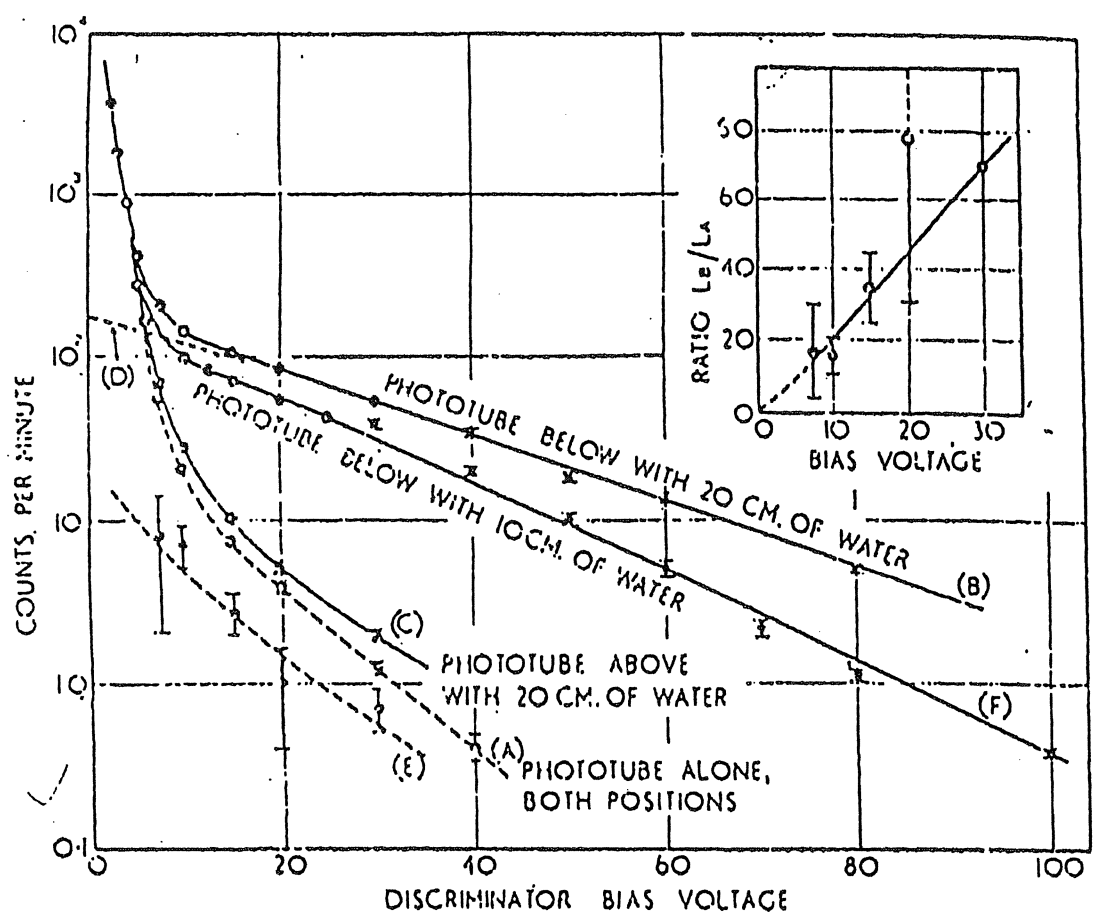


Fig. 4.7. Bias curves obtained by Jelley with the counter shown in Fig. 4.6, to illustrate the directional properties of the radiation.

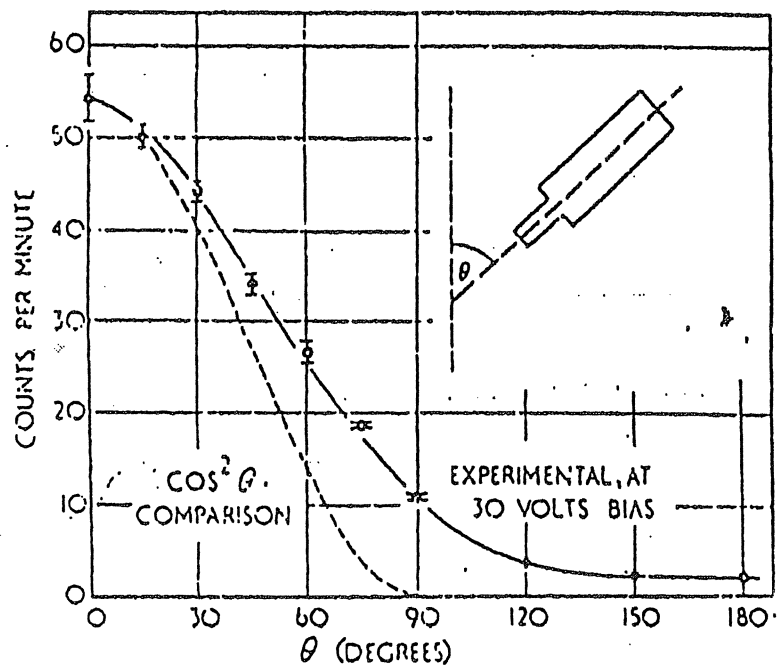


Fig. 4.8. The variation of counting rate with zenith angle, obtained by Jelley with his water detector, Fig. 4.6.

## 5-11. Cerenkov Radiation

A new method of producing visible radiation was discovered by P. A. Cerenkov in 1934. He observed that a beam of fast electrons, such as beta particles from radioactive substances, when moving in a transparent medium caused the emission of visible radiation, provided that the velocity of the electrons was greater than the velocity of light in the same medium. The theory developed by I. M. Frank and I. E. Tamm predicts that the light should be propagated at an angle  $\theta$  to the direction of motion of the electron given by

$$\cos \theta = \frac{c}{\mu v} \quad (5.25)$$

where  $\mu$  is the index of refraction of light and  $v$  the velocity of the electron in this medium. An electron moving through a substance loses most of its energy in ionization and excitation of the atoms. In these processes the electron itself experiences small accelerations and hence radiates energy in the form of electromagnetic waves. Since these waves originate at different points along the path of the electron, radiant energy will be observed only if the waves from the different points reinforce each other. The condition for reinforcement of the waves by interference can readily be derived with the aid of Figure 5-19. The electron beam enters the transparent medium at  $M$  and continues along the path  $MAB$ . The electron radiates energy in all directions from the points along this path. Using the Huygens construction, we obtain the wave front  $BD$ , where the distance  $AD$  is  $ct/\mu$  and  $AB = vt$  where  $t$  is the time taken by the electron to reach point  $B$ . From the figure it follows that the radiation will travel in a direction such that

$$\cos \theta = \frac{c}{\mu v}$$

The Cerenkov radiation was investigated by G. B. Collins and V. G. Reiling (1938), using a beam of electrons of 1.9 Mev energy incident upon a series of thin films of various transparent substances such as glass, water, mica, and cellophane. They photographed the pattern of the emitted light and found the intensity to be a maximum in the direction given by the above equation. They also examined the emitted light spectroscopically and found the spectrum of the Cerenkov radiation to be continuous and to extend from the long wavelength limit of the apparatus usually  $> 5000$  angstroms, down to the ultraviolet absorption limit of the medium in which

(14)

it was produced. H. O. Wyckoff and J. E. Henderson (1943) extended the work of Collins and Reiling to slower electrons, with energies ranging from 240 kev to 815 kev. Using mica as the transparent medium, they obtained results in agreement with the predictions of Frank and Tamm concerning the direction of emission of the Cerenkov radiation.

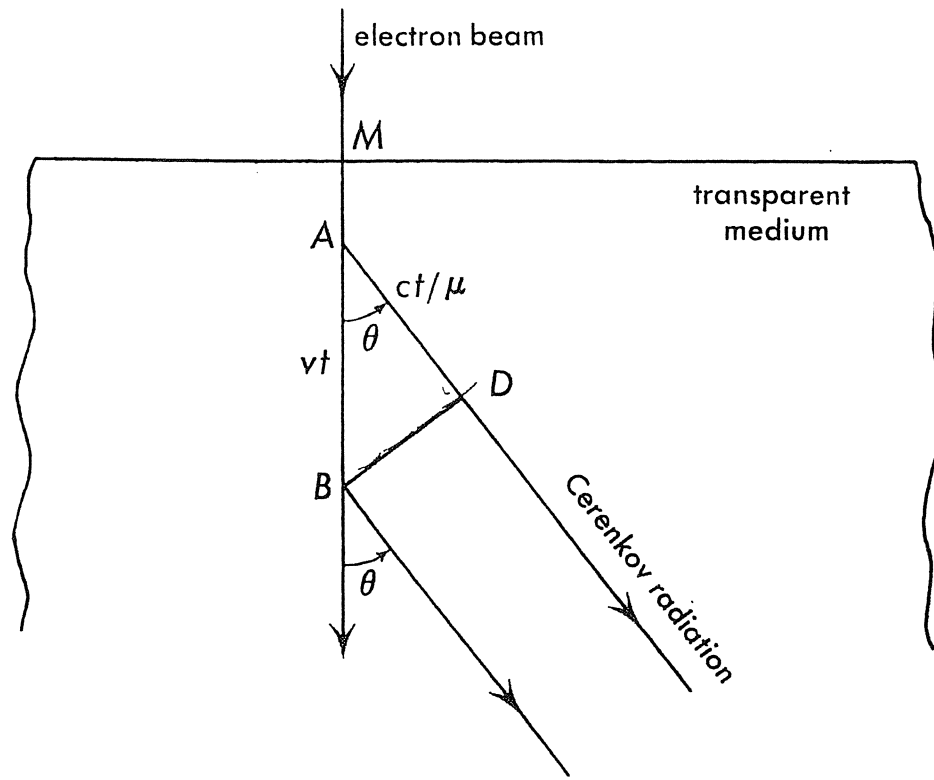


**Fig. 5-19.** Direction of propagation of Cerenkov radiation relative to the direction of motion of the electrons in a transparent medium.

Cerenkov radiation is becoming increasingly useful as a detector of high energy charged particles. The only condition imposed upon these particles is that their speeds be greater than the speed of light in the same medium. In any given medium the angle of emission  $\theta$  is determined only by the velocity of the particle; hence the detection of the Cerenkov radiation is a convenient method for measuring the velocities of high energy charged particles.